

Clusters in the DISPERSE cosmic web

J.D. Cohn^{1,2*}

¹*Space Sciences Laboratory University of California, Berkeley, CA 94720, USA*

²*Theoretical Astrophysics Center, University of California, Berkeley, CA 94720, USA*

6 August 2021

ABSTRACT

Galaxy clusters in a dark matter simulation are matched to nodes in several different cosmic webs found via DISPERSE. These webs are created by varying simulation smoothing and DISPERSE persistence. A few methods are used for DISPERSE node-cluster matching. There are usually many more DISPERSE nodes than clusters and more than one cluster can match the same DISPERSE node. For most matching methods and smoothing $2.5\text{Mpc}/h$ or less, about $3/4$ of the clusters always have a corresponding DISPERSE node. The nearest clusters and DISPERSE nodes within twice the smoothing length of each other obey a cluster mass-DISPERSE node density relation. DISPERSE node matched clusters can also be assigned DISPERSE filaments based upon their corresponding DISPERSE nodes, only about $1/10$ of such cluster pairs frequently have filaments amongst the different DISPERSE webs. The average density profile along a line connecting cluster pairs separated by $< 60\text{Mpc}/h$ is enhanced, with more (on average) counts and mass enhancement for pairs assigned filaments via DISPERSE nodes. Clusters often lacking matched DISPERSE nodes have different trends in their local shear, and perhaps histories, compared to the majority of clusters. It might be interesting to see in what other ways, e.g., observational properties, these clusters differ. The approach here also lends itself to comparing nodes across many cosmic web constructions, using the fixed underlying cluster distribution to make a correspondence.

Key words: cosmology:large scale structure of the Universe, galaxies:clusters

The cosmic web (Bond, Kofman & Pogosyan 1996; Bond & Myers 1996; Pogosyan, Bond & Kofman 1998), exists within many tracers of large scale structure in the universe, from galaxies to dark matter to gas, and underpins the evolution of large scale structure. In the many years since its discovery, numerous ways of characterizing the web and identifying its components (nodes, filaments, voids and walls) have been proposed. Several of these web finders are compared in Libeskind et al (2018), earlier comparisons include, e.g., Leclercq et al (2016); see also the recent meetings (van de Weygaert et al 2016; Higgs Cosmic Web 2019).

In large scale structure, galaxy clusters are the most massive bound structures, and it is common to refer to galaxy clusters as nodes in the cosmic web. This is seen in broad brush, for example, in the web finder comparison of Libeskind et al (2018), most of the clusters lie in cosmic web nodes in all definitions considered. The relation between clusters and the web has been studied for a long time, for instance in the context of the peak-patch algorithm (Bond & Myers 1996), or using the Gaussian field methods of Bardeen et al (1986), also see the review of van de Weygaert & Bond (2008). Clusters have also been used to infer initial conditions, which are then run forward in time to get large scale properties including the cosmic web (e.g., Bos et al 2016; Bos 2016).

In this note, this cluster-node correspondence is explored in more detail, for several DISPERSE webs constructed from a fixed dark matter simulation. The simulation and the web finder DISPERSE are described in §1, as well as a Hessian based node finder used for matching. In §2 a few methods to match clusters and DISPERSE nodes are suggested, applied and compared. Given a DISPERSE node to cluster matching, DISPERSE filaments between nodes can also be assigned to clusters. Properties of these cluster pairs with DISPERSE based filaments are explored in §4 and §5 concludes.

1 SIMULATION DATA AND WEB FINDERS

1.1 Simulation database

The dark matter density map and cluster and galaxy halo (central, satellite and orphan subhalo) samples are taken from the publicly available Millennium simulation (Springel et al 2005) and its database (Lemson & Springel 2006). The simulation corresponds to a fixed time box with side $500\text{Mpc}/h$ and 2160^3 particles; redshift $z = 0.12$ (step 58) is used. The densities (relative to mean) are available in the simulation on a 256^3 pixel grid, with Gaussian smoothing radii of 1.25

* E-mail: jcohn@berkeley.edu

Mpc/h , $2.5 Mpc/h$, $5 Mpc/h$.¹ The commonly used $2 Mpc/h$ smoothing (e.g., Hahn et al 2007a,b) is included by further smoothing the $1.25 Mpc/h$ overdensities. The 2898 halos with $M_{vir} \geq 10^{14} M_{\odot}$ are taken to be clusters². The Planck cosmology (Planck collaboration 2018) Millennium simulation is created from the original Millennium simulation by shifts and scalings (Angulo & White 2010; Angulo & Hilbert 2015), however, the rescaled density field grid is unavailable. So the cosmological parameters are unfortunately outdated ($\Omega_m = 0.25$, $\Omega_b = 0.045$, $h = 0.73$, $n=1$, $\sigma_8 = 0.9$). The particular cosmology is likely irrelevant to the qualitative questions of interest here.

1.2 Finding the web

Many different web finders have been implemented and studied in past decades. The resulting different webs capture different physical aspects and are based upon a wide range of tracers (e.g., dark matter densities, galaxy positions, velocities, etc.) and algorithms, e.g., eigenvalues of the shear tensor (e.g., Zel'dovich 1970; Hahn et al 2007a,b), density critical points and the ridges connecting them e.g., DISPERSE (Sousbie 2011; Sousbie, Pichon, & Kawahara 2011), MMF-2 (Aragon-Calvo et al 2007), NEXUS (Cautun, van de Weygaert & Jones 2013), shell crossing histories and flows (Shandarin & Zel'dovich 1989; Shandarin 2011), phase space ORIGAMI (Falck, Neyrinck & Szalay 2012; Falck & Neyrinck 2015), MWSA (Ramachandra & Shandarin 2015), etc. Twelve approaches were classified, reviewed, applied and compared in Libeskind et al (2018). Using a common $200 Mpc/h$ side dark matter simulation, resulting webs were compared via volume and mass fractions for each web component, overlaps between the same components in different simulations, and more. Webs can also be characterized by node connectivity and angular dependence, studied, e.g., in Gaussian fields and simulations (Codis, Pichon, & Pogosyan 2018), via histories and mergers of critical points (Cautun et al 2014; Cadiou et al 2020), and in terms their relations to many different galaxy properties (there is a very long list, see, e.g., Hellwing et al 2021; Winkel et al 2021). Since the Libeskind et al (2018) comparison paper, methods for web detection (Fang et al 2019; Pereyra et al 2020; Wang et al 2020) and web finder comparison methods (e.g., between filaments Rost et al 2019) have continued to be developed. Each web finding method involves choices of parameters, scales and (sometimes implicitly) other assumptions.

The main web finder used here is DISPERSE (Sousbie 2011; Sousbie, Pichon, & Kawahara 2011)³, a publicly available code which does a multiscale identification of all 4 web components starting with individual objects (such as galaxies) or a density field. Here, DISPERSE is used to identify nodes

and filaments from (Gaussian smoothed) pixel maps of simulation densities relative to the mean.⁴ Using Morse theory, DISPERSE classifies regions using critical points (nulls of the gradient of the field) and integral lines (tangents to the field at every point, which converge at critical points). The DISPERSE web also depends on “persistence”, a parameter describing roughly how much a field has to decrease between two peaks in order for them to be considered as separate peaks. Persistence levels in the examples below are taken to be 1σ , 2σ and 3σ of the density field; although 1σ is a low persistence choice, it helps in examining trends with persistence.⁵ The DISPERSE webs here, based on overdensities in pixels, depend on the pixel scale, the smoothing scale, and the persistence.

One way to associate clusters to a web node is to have the cluster lying “in” the node. In DISPERSE, the nodes are points (dimension zero)⁶ and the filaments are curves (dimension 1), neither of which has associated volume. Two obvious scales for assigning volume are the pixel size and smoothing scale. A third way to associate volume to a DISPERSE node, which uses more information from the density field, is based upon the Hessian based web finder, or “T-web”; some recent descriptions are in Hahn et al (2007a,b). (Other ways of possibly defining the “width” of a DISPERSE node or filament, beyond what will be considered here, include stacking DISPERSE objects (Kraljic et al 2019) or looking at vorticity behavior (Laigle et al 2015).) The Hessian based web finder uses eigenvalues $\lambda_1 \geq \lambda_2 \geq \lambda_3$ of the shear tensor $T_{ij} = \partial_i \partial_j \phi$, where ϕ is the gravitational potential (Zel'dovich 1970). The eigenvalues are calculated for each pixel from the smoothed density field. Every pixel is then assigned a to a web component based on how many eigenvalues are $>$ or $<$ 0, nodes correspond to (+++), filaments to (++-), walls to (+-) and voids to (—). One can generalize to classifying eigenvalues being above or below (Forero-Romero et al 2009) some value λ_{th} , which then becomes an additional model parameter. To construct objects such as a node or filament, from these individually labelled pixels, more assumptions are needed. In the following, every set of contiguous node pixels will be considered a separate Hessian “node” or “patch,” and will be used to assign a volume to DISPERSE nodes within, in order to match the DISPERSE nodes to clusters. Even more assumptions would be required to identify and construct filament objects, which will not be pursued here.

In summary, both the DISPERSE and Hessian classifications depend upon the smoothing length and pixel scale, parameters not intrinsic to the mass distribution itself, DISPERSE

¹ SELECT a.phkey, a.g1.25 from MField..MField as a where a.snapnum=58 order by a.phkey. For larger smoothings, substitute g2.5 and g.5.

² DES.galaxyId, DES.phKey, DES.mvir, DES.x, DES.y, DES.z, DES.type from MPAGalaxies..deLucia2006a as DES where DES.phKey between NNN and MMM and DES.mvir \geq 7300 and DES.type=0 and DES.snapnum=58, where mvir is virial mass of the FOF (linking length 0.2) subhalo.

³ <http://www2.iap.fr/users/sousbie/web/html/indexd41d.html>

⁴ Although DISPERSE can also be used on galaxy counts, the added level of complication became unmanageable in practice for the available computing resources and current data set.

⁵ DISPERSE takes a file of pixel density values, e.g., “pixfile.dat”. One chooses persistence “pers”, which is a number, and runs MSE PIXFILE.DAT -CUT PERS -UPSKL. On that output.up.NDskl one runs SKELCONV OUTPUT.UP.NDskl -OUTNAME PIXFILE -TO NDskl_ASCII to get pixfile.a.NDskl, with node and saddle (filament center) critical points and information about each.

⁶ The allowed DISPERSE node positions on a pixel are at (0, 1/4, 1/3, 1/2, 2/3, 3/4) in pixel units. The pixel size $500/256 Mpc/h$ is used to rescale, and then DISPERSE provided positions are shifted by half a pixel.

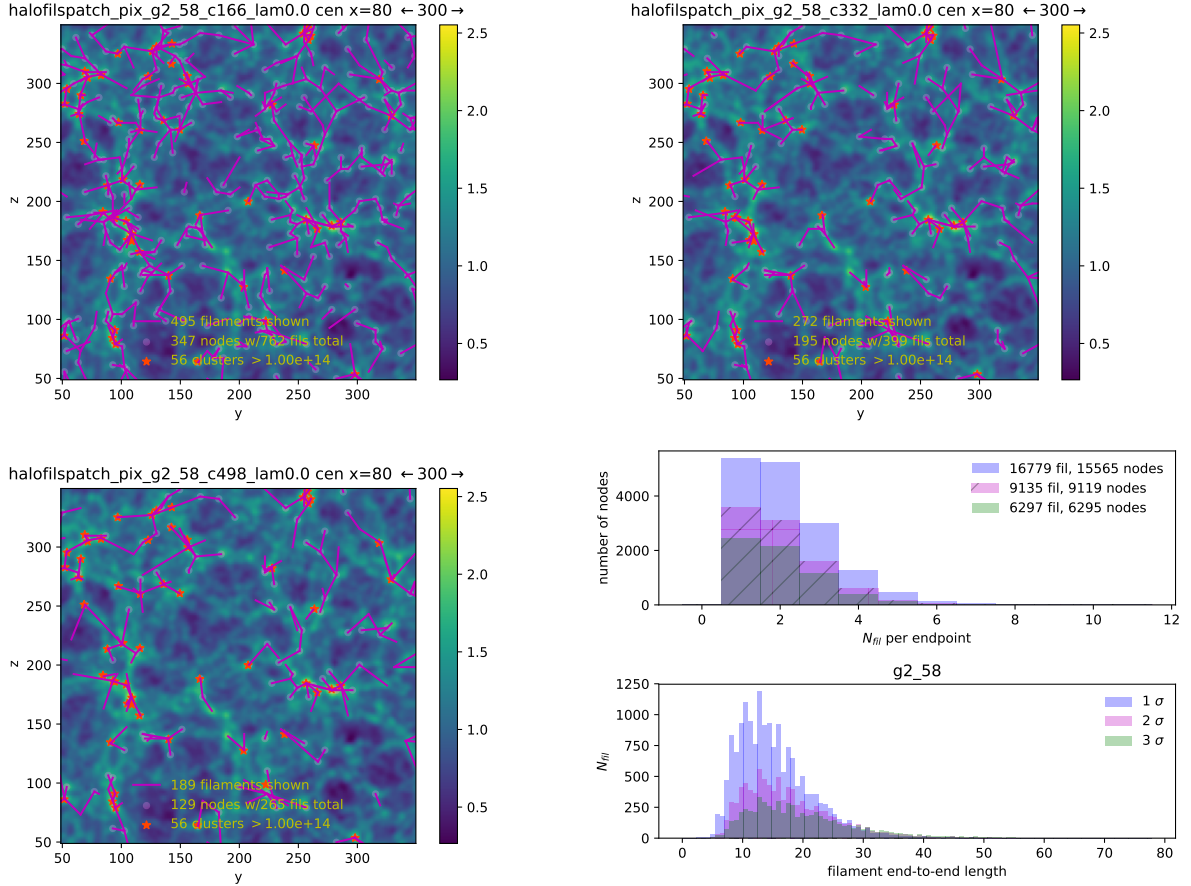


Figure 1. Webs with different DISPERSE persistence levels. Color denotes $\log(\text{density})$. The density slice is $30 \text{ Mpc}/h$ deep and $300 \text{ Mpc}/h$ wide, centered at position $(80, 200, 200) \text{ Mpc}/h$, and viewed down the x axis, with smoothing $2 \text{ Mpc}/h$. The 3 panels show DISPERSE nodes and filaments corresponding to persistence of 1σ (upper left), 2σ (upper right), 3σ (lower left). The grey-blue dots are DISPERSE node pixels, connected by filaments (magenta lines). At lower right are statistics for the full $500 \text{ Mpc}/h$ side box: the number of filaments per node, and distribution of filament lengths. With increasing persistence, the number of nodes, filaments, and connectivity go down, and the average filament length increases.

also depends upon persistence and the Hessian classification also depends upon λ_{th} .

A $30 \text{ Mpc}/h$ deep simulation slice is shown in Fig. 1, with DISPERSE nodes and filaments for persistence 1σ , 2σ and 3σ (the smoothing is $2 \text{ Mpc}/h$). For these three DISPERSE webs, the distribution of DISPERSE node and filament counts, node connectivities, and filament lengths are intercompared in the box at lower right. The 3σ persistence DISPERSE web with smoothing $2 \text{ Mpc}/h$ will be the standard example below. The $2 \text{ Mpc}/h$ smoothing is motivated by its frequent use (e.g., Hahn et al 2007a,b). For all the smoothings considered, as DISPERSE persistence goes up, the number of nodes and filaments go down, as expected, and longer filaments become a higher fraction of all filaments (as the nodes become rarer and further apart). Often the number of filaments does not exceed the number of nodes by very much, with the ratio being very close to 1.⁷

⁷ Within 0.4% except for 1σ persistence, where N_{node}/N_{fil} drops from 98% to 73 % as smoothing increases from $1.25 \text{ Mpc}/h$ to $5 \text{ Mpc}/h$.

2 ASSOCIATING CLUSTERS AND NODES

2.1 Nodes: counts and Hessian node patch properties

In order to associate clusters and nodes, the first question is how many of each are present? This is summarized for several Hessian and DISPERSE choices of parameters in Figure 2. The numbers of nodes are shown at left by circles for DISPERSE persistence of $(1\sigma, 2\sigma, 3\sigma)$ and at right by triangles for Hessian thresholds $\lambda_{th} = (0, 0.5, 1, 2, 3, 4)$. Color denotes the $(1.25, 2.0, 2.5, 5.0) \text{ Mpc}/h$ smoothings. The red dashed line is the cluster number density.

Again, the number of DISPERSE nodes decreases as the persistence is increased, similarly, the number of Hessian node patches decreases as the threshold λ_{th} for eigenvalues to surpass (in order to qualify as a node patch) increases. As mentioned earlier, DISPERSE nodes are single points in a single pixel, parameterized by position and density. The Hessian node patches have, in addition, a size, that is, the number of contiguous pixels classified as nodes. Larger Hessian patches

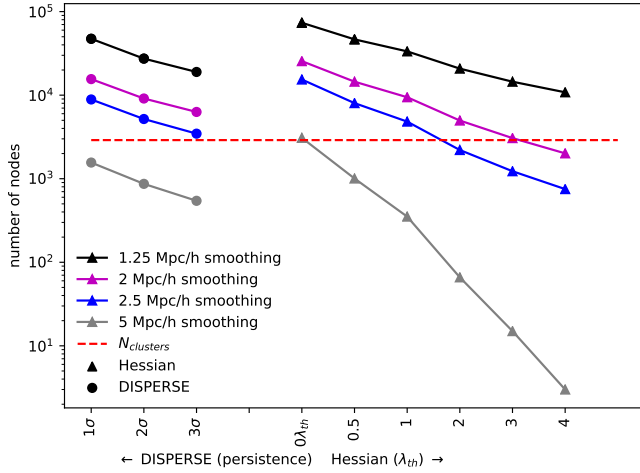


Figure 2. Node counts in different web descriptions vs. the number of clusters, the 2898 halos with $M \geq 10^{14} M_{\odot}$ (red dashed line). For each smoothing (color), the left 3 points are the number of DISPERSE nodes (circles), in increasing persistence. The right 5 points are the number of Hessian nodes (triangles), labeled by λ_{th} (in units of $\partial_i \partial_j \nabla^{-2} \rho / \bar{\rho}$).

are less frequent as the threshold λ_{th} increases and more frequent as smoothing increases.⁸

Looking ahead to matching clusters and DISPERSE nodes lying in the same Hessian node patch, in Fig. 3, the fraction of DISPERSE nodes lying in Hessian pixels is shown as a function of threshold λ_{th} and DISPERSE persistence. As the DISPERSE persistence is raised, a higher fraction of DISPERSE nodes lie in Hessian node pixels for a given λ_{th} , that is, the definitions tend to overlap more often. Given the steep drop in number of matched DISPERSE nodes to Hessian patches as λ_{th} is raised, in order to have more DISPERSE nodes available to match to clusters, only $\lambda_{th} = 0$ Hessian patches will be used hereon. As smoothing increases, a smaller fraction of DISPERSE peaks lie in Hessian patches for a given λ_{th} .

For clusters in Hessian node patches, most Hessian nodes have no clusters at all. However, a few Hessian node patches contain several clusters, leading to a “node occupation distribution”, shown for the four different Hessian web smoothings (again, $\lambda_{th} = 0$) in Fig. 3, bottom. More clusters share Hessian patches and more clusters are missed as the smoothing increases (legend, Fig. 3, bottom).

2.2 Associating clusters to nodes

A correlation between clusters and DISPERSE nodes is expected, but the relation is not necessarily expected to be one to one. In particular, the DISPERSE web finds peaks (nodes, with a height difference requirement depending on persistence) and ridges (filaments), and depends upon smoothing and pixel scales as well. Clusters have integrated density

⁸ For $\lambda_{th} = 0$ and smoothing 1.25 Mpc/h , 40% of the Hessian nodes have only one pixel, while for the more restrictive $\lambda_{th} = 4$, 71% of the Hessian nodes only have one pixel. As smoothing increases, fewer node patches have only one pixel, e.g., only 3% do so for smoothing 5 Mpc/h and $\lambda_{th} = 0$.

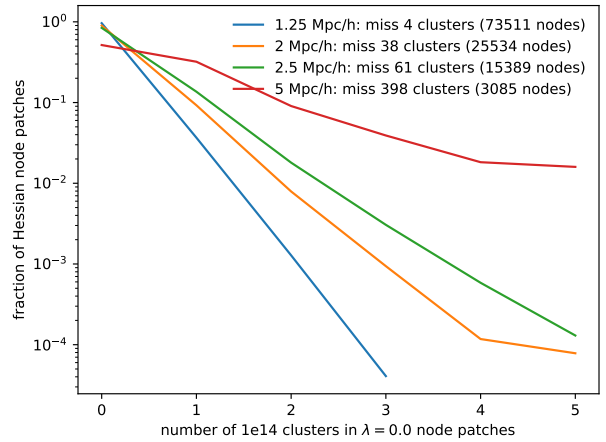
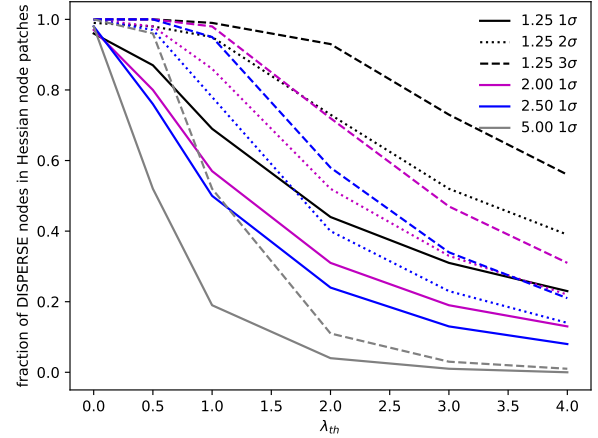


Figure 3. Top: DISPERSE nodes corresponding to Hessian nodes (via lying in a shared pixel), by DISPERSE persistence: 1σ (solid), 2σ (dotted), 3σ (dashed), with color giving Gaussian smoothing of 1.25 Mpc/h , 2 Mpc/h , 2.5 Mpc/h , 5 Mpc/h as indicated. A higher fraction of higher persistence or lower smoothing DISPERSE nodes have Hessian matches for fixed λ_{th} . Bottom: the fraction (note the log scale) of Hessian node patches $\lambda_{th} = 0$ with a given number of clusters, as a function of smoothing. The Hessian patch nodes significantly outnumber the clusters except for the 5 Mpc/h smoothing. The numbers of missed clusters (out of 2898) are shown in the legend.

above some absolute scale (mass scale), and do not depend upon the smoothing and pixel scales.

Several ways to associate clusters to the DISPERSE nodes were considered and are compared below:

- “patch”: if the cluster center pixel is in the same Hessian node patch as the DISPERSE node pixel
- “fixed” and “nearest”: if, for a given DISPERSE nodes, the cluster center is within some fixed distance of (“fixed”), or is the nearest cluster center (“nearest”) within that fixed distance, taken to be twice the smoothing
- “pix”: if the cluster center and the DISPERSE node lie in the same pixel

Other matching methods using Hessian patches were con-

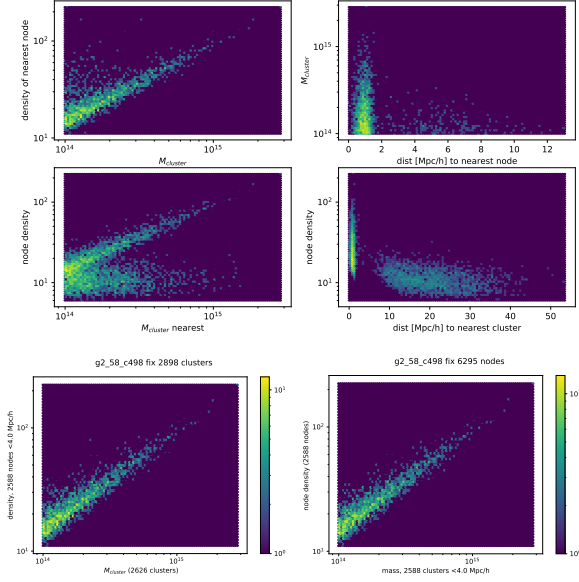


Figure 4. Relation between clusters and their nearest DISPERSE node, for 3σ persistence and smoothing $2 \text{ Mpc}/h$. At top, the nearest node for each of the 2898 clusters is considered. The low mass clusters are paired with nodes having a range of densities, and sometimes that association is weak, as the nearest node can be up to $15 \text{ Mpc}/h$ away. Within twice the smoothing distance ($4 \text{ Mpc}/h$), 9% of clusters do not have a DISPERSE node. At middle, the nearest cluster for each of the 6295 DISPERSE nodes is considered (there are many more nodes than clusters), which are sometimes $> 40 \text{ Mpc}/h$ away. 59% of the 6295 DISPERSE nodes do not have a cluster within $4 \text{ Mpc}/h$. The lowest density nodes have a wide range of paired cluster masses. More than one cluster can have the same nearest DISPERSE node and vice versa. The color scheme for densities in each plot pixel is logarithmic. Bottom: restricting to DISPERSE node-cluster pairs within twice the smoothing length, a cluster mass-DISPERSE node density is seen. At left, fixing the 2898 clusters and finding the closest DISPERSE node, at right, vice versa.

sidered, such as clusters being within a set distance from a Hessian node patch center or peak, or a distance from any pixel in a Hessian node patch, but all of these introduce more complexity, assumptions and difficulty in interpretation.

For matching clusters to DISPERSE nodes based upon distance (“fixed” and “nearest”), the choice of distance scale was guided by looking at the distance to the nearest DISPERSE node for each cluster (e.g., Fig. 4, upper right) and the distance to the nearest cluster for each DISPERSE node (Fig. 4, middle right), shown for the reference DISPERSE web with $2 \text{ Mpc}/h$ smoothing and 3σ persistence. For all smoothings, there seems to be a clear subset of clusters with a DISPERSE node close by, roughly captured by using twice the smoothing scale as a distance cutoff.⁹ Restricting to only DISPERSE node-cluster pairs within twice the smoothing length,

⁹ The pixel scale of $\sim 2 \text{ Mpc}/h$ seems relevant, as DISPERSE nodes are only defined on a grid with that resolution, i.e., DISPERSE node location changes on smaller scales do not reflect the underlying matter distribution on smaller scales. It was not clear how to take this into account.

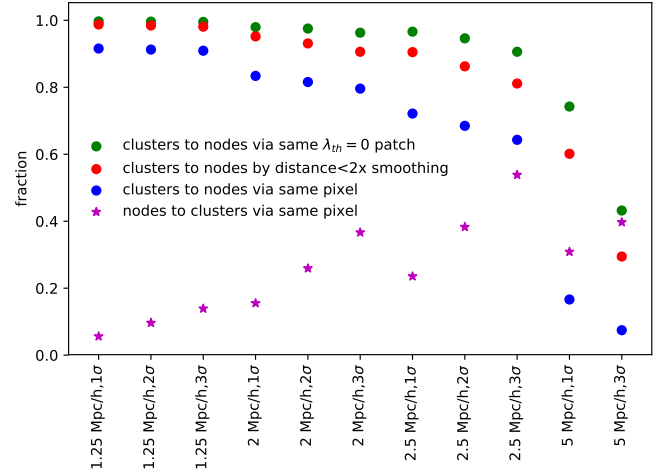


Figure 5. Fractions of clusters matched to DISPERSE nodes via the “nearest/fixed”, “pix”, “patch” methods, as a function of smoothings and persistence (1σ , 2σ , 3σ) and methods; clusters lying in the same $\lambda_{th} = 0$ Hessian patch (green dots, “patch”), red: lying within a distance of twice the smoothing length (red dots, “nearest” or “fixed”), and lying within the same pixel (blue dots, “pix”) as a DISPERSE node. The $\lambda_{th} = 0$ Hessian patch and the DISPERSE 1σ persistence $1.25 \text{ Mpc}/h$ smoothed nodes gives the most matched clusters (2889/2898). The “patch” method for higher λ_{th} values have fewer clusters matching DISPERSE nodes relative to all 3 methods shown. Stars refer to fractions of DISPERSE nodes with clusters in the same pixel, matching via the “pix” method, a similar fraction (from 94% to 29%) of DISPERSE nodes do not have a cluster within $2 \text{ Mpc}/h$.

a DISPERSE node density-cluster mass relation is seen all the way down to the lowest DISPERSE node densities and cluster masses.

More than one cluster can have the same nearest DISPERSE node and vice versa. The number of times the closest DISPERSE node to a cluster within the (twice smoothing) distance cut is already matched is < 25 for the $1.25 \text{ Mpc}/h$ smoothing, dropping to 5 additional clusters for $2 \text{ Mpc}/h$ smoothing with 1σ persistence and then becoming zero for larger smoothings or persistence. In contrast, the number of DISPERSE nodes whose nearest cluster is already matched rises with smoothing ($\sim 1, \sim 40, \sim 110, > 300$) for smoothings ($1.25 \text{ Mpc}/h$, $2 \text{ Mpc}/h$, $2.5 \text{ Mpc}/h$, $5 \text{ Mpc}/h$). Both “patch” and “fixed” also do not necessarily associate a unique cluster to a given DISPERSE node (or a unique DISPERSE node to a given cluster, for patch), as they map all clusters in a given region to the same DISPERSE node.

The pixel matching method is unambiguous but can fail to match a cluster to a DISPERSE node if the cluster center is offset from the pixel containing the latter, even if the cluster itself extends into the DISPERSE node pixel.

Although for almost all DISPERSE webs there are many more DISPERSE nodes than clusters, not all clusters are matched to DISPERSE nodes. The fraction of clusters which are matched to DISPERSE nodes by each of the 4 methods above¹⁰, for the different DISPERSE webs, is shown in Fig. 5.

¹⁰ Note that “nearest/fixed” are two methods, in one case only

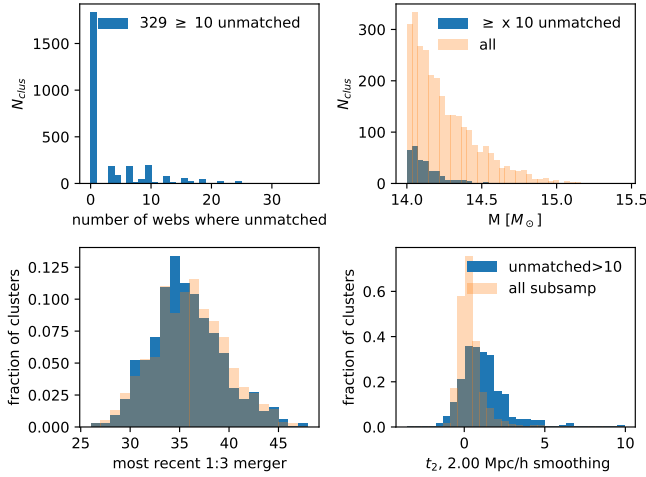


Figure 6. Properties of clusters unmatched in 10 or more of the 36 combinations of DISPERSE webs and cluster matching methods (smoothing $< 5 \text{ Mpc/h}$). Upper left is the number times each cluster is unmatched for the 36 combinations. Upper right shows the full cluster mass distribution and the unmatched (darker color) cluster mass distribution, which tends to be lower mass. Lower left and right compare a samples of matched clusters with the same mass distribution s (lighter) and the 329 clusters unmatched ≥ 10 times. At lower left, the most recent 1:3 merger time step is perhaps slightly less recent for unmatched clusters (more recent is higher number). At lower right, $t_2 = \lambda_2 - \delta/3$ (calculated for smoothing 2 Mpc/h) seems higher for the unmatched clusters t_2 . Similar trends were seen for the smaller number of clusters which remained frequently unmatched when dropping matching via “pix”.

In contrast to the large number of matched clusters, most of the DISPERSE nodes are not matched to clusters (for example, stars in Fig. 5, for “pix” matching), although going to low enough halo mass would perhaps give at least one halo in the same pixel as every node. Increasing the fraction of matched DISPERSE nodes by raising persistence or smoothing causes the number of matched clusters to decrease.

Setting aside the two 5 Mpc/h smoothed webs for the rest of this section, as their DISPERSE nodes miss significantly more clusters, there are 36 combinations of DISPERSE webs and matching methods. For these, the statistics of unmatched clusters are shown in the upper left hand corner of Fig. 6. Over half of the clusters (1832/2898) were matched to DISPERSE nodes for every web and method. Dropping the “pix” method, 9 cases and the most restrictive way to match clusters and DISPERSE nodes, 2248/2898 clusters, about 3/4, were always matched to DISPERSE nodes, by all remaining 3 methods.

One cluster was missed by every method, by dint of being slightly beyond the cutoff of twice the smoothing scale, while 79 (329) were not matched to DISPERSE nodes for 20 (10) or more web/method combinations (out of 36). Some characteristics of the 329 clusters which were unmatched for 10 or more times are shown in Fig. 6. At upper right is their mass

one DISPERSE node is matched, in the other, all DISPERSE nodes within twice the smoothing are matched. For counting how many clusters have at least one match, these give the same result, and so are shown as the same point.

distribution (they tend to be lower mass). At lower left is the time of their most recent major (1:3) merger, which seems slightly earlier than for a random cluster subsample with the same mass distribution, compared to the unmatched clusters. For different underlying DISPERSE webs, the merger history difference is most pronounced for the smallest smoothing and increases as the maximum allowed distance for matching between clusters and DISPERSE nodes increases from twice the smoothing scale. At lower right is the distribution of unmatched versus a random subsample with the same mass distribution, for the middle component of “velocity shear” (Ludlow & Porciani 2011), $t_2 = \lambda_2 - \delta/3$ in the cluster pixels. The t_2 distribution of the frequently unmatched clusters seems to be higher relative to the subsample of all clusters. (When considering clusters unmatched for a specific DISPERSE web matching, t_2 is calculated using the same smoothing scale as the DISPERSE nodes. Here 2 Mpc/h is considered.) The “velocity shears” t_i , refer to whether local collapse is favored (if > 0) or impeded (if < 0) along a given axis, and these unmatched clusters seem to be in regions that have collapse favored along two axes more frequently ($t_2 > 0$) relative to all clusters. More frequent $t_2 > 0$ was also found for the initial conditions of “peakless halos”, massive halos lacking a corresponding high mass peak in the initial conditions (Ludlow & Porciani 2011). The difference in t_2 between matched and unmatched clusters is largest for webs with smaller smoothing and for matching methods which produce fewer unmatched clusters. Again, samples of clusters which are further away from the nearest DISPERSE nodes furthest away tend to have the highest difference in t_2 from the matched clusters. For nodes, the unmatched DISPERSE nodes also tend (slightly) to be lower mass for some smoothings and persistences, but it is harder to look at trends across different webs as the DISPERSE nodes themselves also vary between webs.

In summary, DISPERSE nodes can be matched to clusters in several ways. For the 9 DISPERSE webs with smoothing $< 5 \text{ Mpc/h}$, over half of the clusters always have a matched DISPERSE node, and over 3/4 of the clusters have a DISPERSE node match excluding the “pix” matching method, exact pixel overlap of DISPERSE nodes and cluster centers. The clusters without DISPERSE nodes in at least 10 of the 36 matching methods and underlying DISPERSE webs, $\sim 11\%$, tend to be lower in mass, have perhaps a earlier most recent major merger, and a higher t_2 than the full cluster sample. (Similar results were found for the 1/4 clusters which didn’t always have a DISPERSE node match for the “fixed”, “nearest”, and “patch” methods.) Clusters and DISPERSE nodes within twice the smoothing length of each other have a DISPERSE node density-cluster mass relation.

3 CLUSTER-CLUSTER FILAMENTS

3.1 Assigning filaments

The four methods above associate DISPERSE nodes and galaxy clusters. As the DISPERSE nodes are linked by DISPERSE filaments, clusters can be assigned filaments, “linked”, based upon their matched DISPERSE nodes. There will be 4 filament assignments for each underlying DISPERSE web, due to the 4 ways of matching clusters to DISPERSE nodes.

Filaments are assigned to clusters in the following way.

First, filaments in the full DISPERSE web are restricted to the cluster-matched DISPERSE nodes. DISPERSE nodes with no associated cluster are marked to be dropped and then sorted according to the number of filaments they have. Going from unmatched DISPERSE nodes with the fewest to the most filaments, any filaments where both ends are cluster matched DISPERSE nodes are kept. In addition, any pair of filaments meeting at the same unmatched DISPERSE node, with an angle of more than 120 degrees, is replaced by a single filament bypassing the unmatched node, after which the unmatched node is dropped. This is to catch the cases where two cluster matched DISPERSE nodes are linked via an intermediate unmatched DISPERSE node without very much bending at the node. This is repeated until all unmatched nodes are gone. Unmatched nodes with just one filament are simply dropped. This produces a map of only cluster matched DISPERSE nodes and their filaments. (A second map was also made, where only filaments between matched DISPERSE nodes were kept, dropping the cases where interpolation was done when dropping an unmatched DISPERSE node. Unless specified otherwise below, the cluster-cluster filaments below include those found via interpolation.)

The next step is to replace DISPERSE nodes which are connected by filaments with their matched clusters. Because the cluster to DISPERSE node matching is not always one to one, this step can be ambiguous. A matched node might have two clusters associated with it, or two matched nodes might have the same nearest cluster. (The number of occurrences of multiple clusters within a single Hessian node patch, used in the “patch” method was shown in Fig. 3, at bottom.) Again, matching the nearest cluster and DISPERSE node within a smoothing dependent distance cut can also lead to degeneracies because the nearest DISPERSE node to a cluster might not be the nearest cluster to that DISPERSE node. Two options are used, and appear to give similar results. In one case, “nearest,” if two clusters both have the same nearest node, within the distance cutoff, they are linked to each other with filaments, and if two nodes claim the same cluster as their nearest cluster, and another cluster claims either node, the two clusters are also linked via filaments. A second way to proceed, “fixed dist,” is to match every cluster within the smoothing dependent distance cut to the node, and if there is more than one, to connect these clusters to each other with filaments.

At the end of this construction, every cluster has a list of other clusters to which it is connected via filaments. There is a different set of cluster-cluster filament pairs for each combination of cluster-DISPERSE node matching method and underlying original DISPERSE web.

3.2 Comparing different cluster-cluster filament assignments

An underlying DISPERSE web is shown along with two cluster pair filament assignments based upon in Fig. 7. As in Fig. 1 this is for a 30 Mpc/h density slice, with the original DISPERSE web at upper left (magenta filaments, smoothing 2 Mpc/h with 3σ persistence), and the “nearest” method filaments at upper right and the “patch” method filaments at lower left (cluster DISPERSE node matching methods are described in §2.2). The matched clusters are red stars, unmatched clusters are yellow stars, and the cluster-cluster filaments

are shown as black lines. At lower right are the statistics of all the filament assignments based upon this particular DISPERSE smoothing and persistence.

Included in the comparison of cluster-cluster filament pairs in Fig. 7 (lower right panel) is a cluster based minimal spanning tree web (some variants are in, e.g., Barrow et al (1985); Park & Lee (2009); Alpaslan et al (2014); Pereyra et al (2020)). This is included for comparison because it is a web constructed directly from the clusters themselves, by choosing each cluster as a web node. It is created by ranking cluster pairs according to some property (two ranking properties which have been used for halos are the distance between them, Alpaslan et al (2014), used here, or $M_1 M_2 / r^2$ Pereyra et al (2020)). Filaments are then assigned to cluster pairs in ranked order, omitting any pair where both proposed endpoints are already connected to filaments, to get $N_{clus} - 1$ filaments.

In the filament assignments for the underlying 2 Mpc/h smoothing, 3σ persistence DISPERSE web, shown in Fig. 7, some general trends can be seen. As the cluster-cluster filament pairs only have 2898 clusters to serve as possible endpoints, versus the 6295 original DISPERSE web nodes, there are fewer cluster-cluster filaments (filament counts are listed in the legend of Fig. 7, top half of lower right panel). There are also some longer cluster-cluster filaments relative to those of the underlying DISPERSE web, likely due to the merging of shorter filaments when interpolating between matched DISPERSE nodes. The filaments tend to be relatively shorter in the cluster based minimal spanning tree web, as the shortest distance pairs were chosen to have filaments.

More generally, in the original DISPERSE webs, and the minimal spanning tree webs, every cluster has at least one filament (although the minimal spanning tree web tends to be more tree than “web” like, as it does not have closed loops). The cluster-cluster filaments do not result in a completely connected object, and of course, there are also clusters with no filaments, either because they have no associated DISPERSE nodes (see Fig. 5) or because their matched DISPERSE node didn’t have filaments to another matched DISPERSE node. Considering all the cluster-cluster filament pairs, based upon all the different DISPERSE webs, the fraction of clusters with no filaments is highest for pixel matching (“pix”), and lowest for Hessian node patches (“patch”). For “patch”, “nearest”, “fixed dist,” for smoothing below 5 Mpc/h , the fraction of clusters with no filaments, for both reasons, combined, lies between $\sim 15\%$ – $\sim 25\%$, with the number of unlinked clusters dropping to $\sim 10\%$ for the 2.5 Mpc/h smoothing, while for “pix” the number of unlinked clusters was above 30% for all smoothings. The 5 Mpc/h smoothing reached 95% unlinked clusters (for “pix”) and more generally was worse for linking clusters for all methods. In the 36 cases with smoothing $< 5 Mpc/h$, 47 of the 2898 clusters are never connected via a filament to another clusters. If filaments aren’t interpolated across unmatched DISPERSE nodes, this goes up to 152 clusters.

4 CLUSTER PAIRS

4.1 Cluster pairs with and without filaments

All of these sets of induced cluster-cluster filaments, from each of the 36 DISPERSE web-matching combinations, start

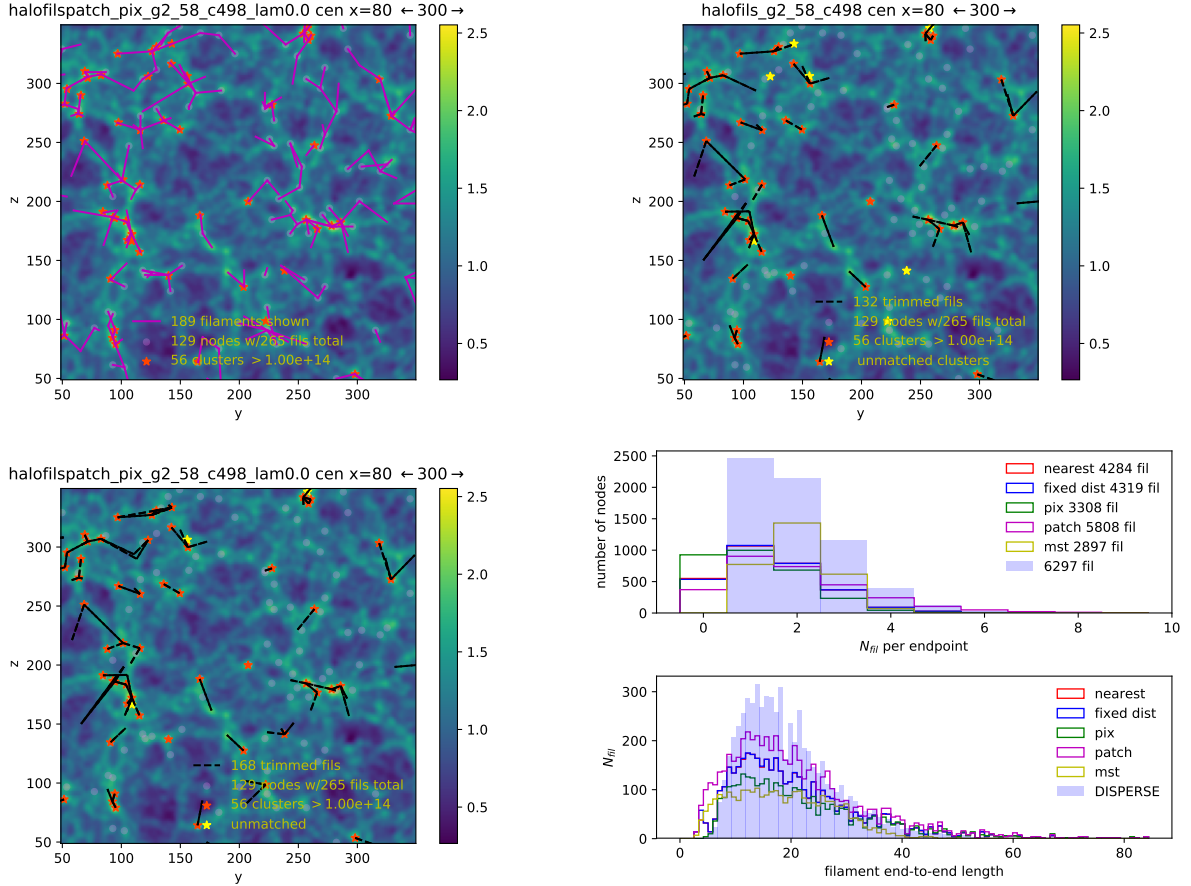


Figure 7. Comparisons of a 30 Mpc/h slice for filaments resulting from the 3σ persistence, 2 Mpc/h smoothed DISPERSE web, overlaying a (logarithmic) density map (from Fig. 1). Interpolation through unmatched DISPERSE nodes is done as described in the text. At upper left is the original DISPERSE web. The filament endpoints are DISPERSE node pixels, connected by DISPERSE filaments (magenta). The red stars are clusters. For the cluster-cluster filaments, unmatched clusters are yellow stars, and the black lines show cluster pairs which are connected by using their matched DISPERSE nodes and either the “nearest” method (upper right) or “patch” method (lower left), described in §2.2. Log scale is used for density. At lower right are statistics for all the different matching methods described in §2.2 plus the cluster based minimal spanning tree (“mst”) described in the text: number of filaments per cluster at top (with total filaments per method in the legend) and filament length distribution at bottom. All maps have the same filament endpoints (clusters) and original fixed underlying DISPERSE web (its statistics are shown as shaded bars, repeated from Fig. 1). Clusters can have no filaments due to being unmatched to a DISPERSE node or by having their matched DISPERSE node not connected by filaments either directly or via interpolation to other cluster-matched DISPERSE nodes.

with the same set of clusters. One way of thinking about the cluster-cluster filaments which appear based upon a particular matching method and underlying DISPERSE web is as an operation on the distribution of cluster pairs, choosing which are linked. (Given the huge numbers of clusters with no filaments when 5 Mpc/h smoothing is used, these DISPERSE webs and their associated cluster-cluster filament pairs will not be discussed in this section.)

Of the over 420,000 cluster pairs in the box, only 5849 pairs have a filament in any of the 36 webs. If interpolation is dropped, that is, only underlying DISPERSE web filaments with both ends lying on cluster matched DISPERSE nodes are kept, only 4440 of these filaments remain. The distribution of how often each pair appears in these 36 webs is shown in Fig. 8. Of these, 384 cluster pairs had filaments in every web, and these tended to be at smaller separation, e.g., between 10-20 Mpc/h , although one cluster pair which always

had a filament was separated by 65 Mpc/h . Fewer than 1/5 of the total number of pairs ever linked have filaments in at least 3/4 of the 36 persistence/smoothing/matching combinations (only roughly half of the 1/5 frequently linked cluster pairs correspond to filaments directly, not interpolated, between two cluster matched DISPERSE nodes). About 1/3 of the cluster pairs ever having filaments only have them rarely, i.e. for ≤ 4 of the combinations, while half have filaments for ≤ 9 of the 36 persistence/smoothing/matching combinations. In this way, the 36 ways of assigning filaments to cluster pairs produce 36 sets of mostly non-coinciding cluster pairs with filaments. The rarest pairs seem to occur for “patch” matching, and for the largest smoothing.

Some trends appear in the pairs of clusters which are linked by filaments. As might be expected, clusters which are closer together are more likely to have a filament between them. In more detail, for these 36 webs, the fractions of cluster pairs

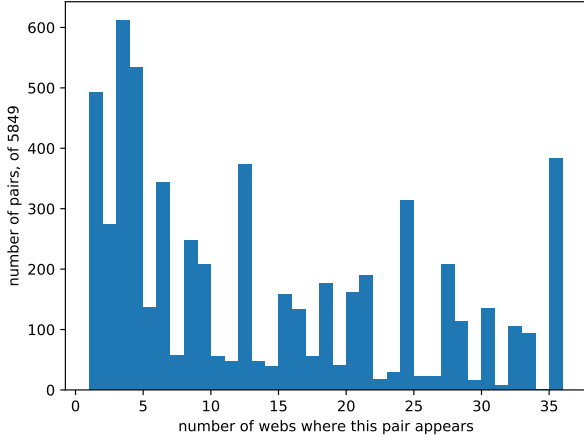


Figure 8. Frequency of cluster pairs with filaments. The number of times a given cluster pair has a filament, out of the 36 persistence/smoothing/matching combinations; 384 pairs had filaments in all 36. Only the 5849 pairs with a filament in at least one of the 36.

which are connected by a filament, as a function of separation, are shown in Fig. 9. A dip in probability for somewhat close pairs is noticeable for the “nearest” and “fixed dist” restricted webs, for smoothings 2, 2.5 Mpc/h , although it is slightly present in the “patch” web as well.¹¹ For a given separation bin, cluster pairs with filaments were a minority of cluster pairs beyond 15–20 Mpc/h separations for any given separation.

Pair separation is the strongest indicator of whether a cluster pair is likely to be linked (but not sufficient information, as seen in Fig. 9). Alignments of the clusters’ long axes are another property that is expected to make a filament more likely Bond, Kofman & Pogosyan (1996); Bond & Myers (1996). Taking pairs with separation less than $\sim 50 Mpc/h$, the fraction of linked pairs did not seem to have a strong dependence upon cluster-cluster axes alignment (e.g., bottom of Fig. 10, for 2 Mpc/h smoothing and 3 σ persistence). However, when the cluster-cluster pair axis was aligned with either cluster axis, a filament was present around twice as often as when these two axes were perpendicular to each other (although still only $\leq 25\%$ of the time, largest for the largest smoothing), some examples are shown in Fig. 10, at top. (For both the cluster-pair and cluster-cluster alignment distributions, the distribution of angles for the full set of pairs, again, up to $\sim 50 Mpc/h$ was approximately flat.)

Instead of looking at pair features one-by-one to see if a filament is present, machine learning can try to answer the clas-

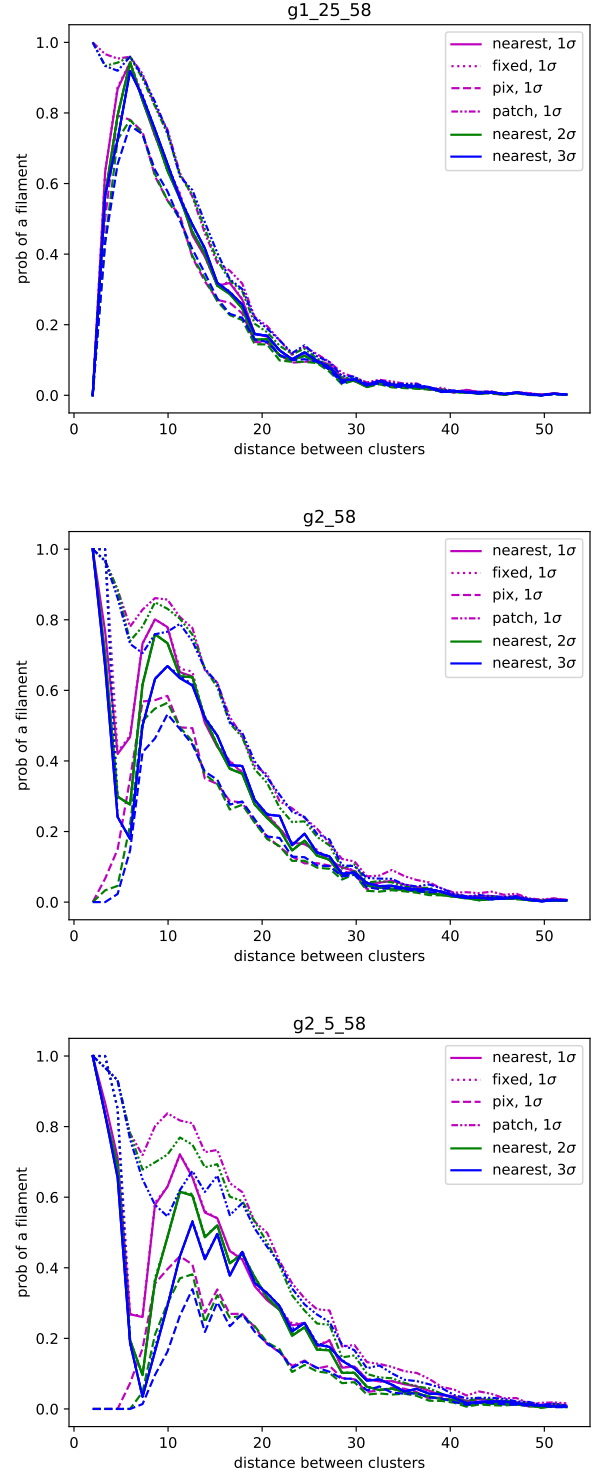


Figure 9. Probability of having a filament between two clusters as a function of cluster separation, for different smoothing lengths (1.25 Mpc/h , 2 Mpc/h , 2.5 Mpc/h top to bottom). Line types distinguish cluster-DISPERSE node correspondence, color denotes chosen DISPERSE persistence. The Hessian patch matching between clusters and the DISPERSE web gives the simplest relation between filament likelihood and cluster separation, roughly less likely as separation increases, although for all webs based on smoothing above 1.25 Mpc/h there are additional features as a function of cluster separation.

¹¹ As clusters matched to the same DISPERSE node are linked by filaments, increasing the radius within which clusters and DISPERSE nodes are matched would remove the drop in number of linked cluster pairs, however, this dip is at the scale where nearby clusters tend to appear, so changing the matching radius would also tend to match more cluster pairs to a single DISPERSE node. Another possibility is to add yet another parameter in creating the restricted web for “nearest” and “fixed”, a separate minimum radius within which all clusters are linked.

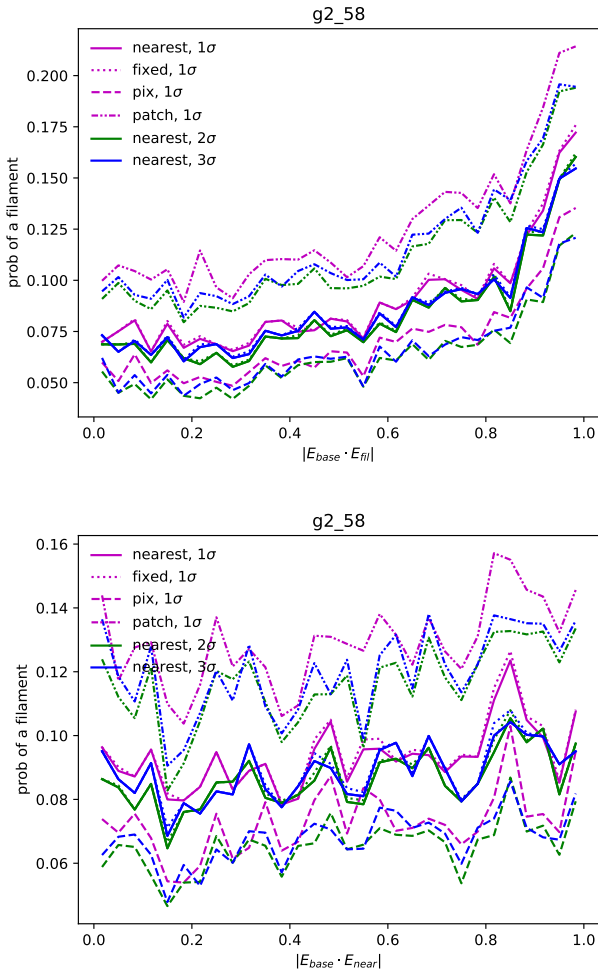


Figure 10. Fraction of cluster pairs separated by less than ~ 50 Mpc/h which have a filament, for different cluster to node matching methods as described in §2.2. Top: as a function of alignment of a cluster axis and cluster-cluster pair axis. Bottom: as a function of alignment of the two cluster pair endpoints. Smoothing length for both is $2 Mpc/h$. Again, line types distinguish cluster-DISPERSE node correspondence, color denotes chosen DISPERSE persistence. The distribution of all cluster pair alignments or cluster-pair axis alignments, irrespective of a filament being present, seems approximately flat.

sification problem (given a pair, is there a filament present or not) using a combination of features. Some methods also assign “importance” of each feature to the classification. Using the Random Forest classifier, “out of the box”¹², the relative importance of the features of distance, cluster-pair axis alignment, cluster-cluster alignment, and rank, i.e. how many clusters were closer to the endpoint cluster than the other endpoint of the pair, were considered for all pairs below a fixed separation $\sim 50 Mpc/h$. Pair separation was, as expected, the most “important” feature, followed by rank (highly correlated

with pair separation). When considered along with pair separation, cluster-cluster alignment and cluster-pair axis alignment were both approximately of the same “importance,” in contrast to the differing dependence seen when these were considered on their own in Fig. 10. It is possible that considering cluster alignment separately from cluster separation, as in Fig. 10, weakened the signal. It is also true, however, that for many cases, the machine learning success of matching filaments to pairs was not that good (above 8% mismatch for 11/36 of the filament assignments), so it might be that more tuning is needed to use this approach, or that the the presence of a filament is not amenable to being predicted by these (few) parameters. The AdaBoost classifier was also tried¹³, but did quite poorly on some of the 36 restricted webs.

4.2 Halo and mass density between cluster pairs

One property of cluster pairs is the radial density profile perpendicular to the cluster-cluster pair axis. If the cluster pair is connected by a filament, this is the filament radial density profile. The average of this profile per unit length, for all cluster pairs up to some maximum separation, is shown in Fig. 11 for the (21940, 37282, 58702) cluster pairs with separations less than ($40 Mpc/h$, $50 Mpc/h$, $60 Mpc/h$), respectively, either counting (left panel) or weighing (right panel) all galaxy halos above ($10^{11} M_\odot$, $10^{12} M_\odot$, $10^{13} M_\odot$), as indicated. Again, galaxy halos can be either central, satellite or orphan subhalos in the Millennium Simulation. Pairs separated by more than $60 Mpc/h$ are omitted, ranging from 0.3% to 6% of the restricted web cluster pairs with filaments. As can be inferred from Fig. 9, these omitted filament pairs are a very small fraction of large separation pairs. (Larger fractions of long filaments appeared with larger web smoothings.) Dividing each average profile by its peak count density, the profiles become approximately self similar (Fig. 11, bottom) for the two lower minimum halo masses together, or the highest minimum mass samples, separately. The peak density increases when restricting to closer pairs (as closer pairs, see Fig. 9, are more likely to have filaments), or including more (i.e., lower mass) halos.

Restricting to cluster pairs with filaments, the profiles for an underlying DISPERSE web with $2 Mpc/h$ smoothing, 3σ persistence, matched to clusters via “patch,” are shown in Fig. 12. Cluster pairs linked through an unmatched DISPERSE node via interpolation are either kept (“c” fils) or dropped (“dir c” fils), the two profiles are not that different. Also shown is the average profile between all cluster pairs with the same maximum separation and halo minimum mass, and the corresponding stacked perpendicular profile for the cluster pairs without a filament (slightly lower than the average). The DISPERSE node pair profile, dotted line, is discussed below. The counts and mass profiles for filament pairs (solid lines) are steeper than the corresponding average pair profiles with the same length and halo mass constraints (dashed lines), although in many of the 36 web-matching combinations the two curves converge before reaching radius $10 Mpc/h$. The average cluster filament pair tended to follow an approximately $1/r$ profile for $> 2 Mpc/h$, less steep than

¹² RandomForestClassifier(max_depth=5, n_estimators=10, max_features=1), imported from sklearn.ensemble, described in <https://scikit-learn.org/stable/modules/ensemble.html>

¹³ AdaBoostClassifier(), also from sklearn.ensemble

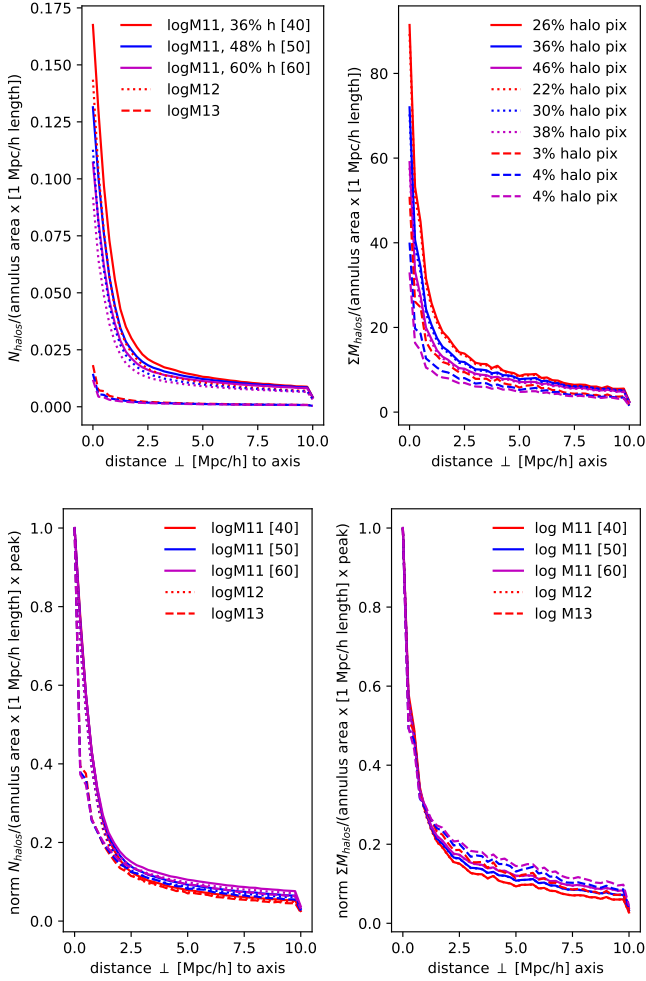


Figure 11. Enhanced density of galaxy halo counts (left) or their mass (right), between cluster pairs, for halo masses above $10^{13} M_{\odot}$ (dashed), $10^{12} M_{\odot}$ (dotted) and $10^{11} M_{\odot}$ (solid). Top: the radial galaxy number density (left) and halo mass density (right) perpendicular to the line linking all pairs of neighboring clusters separated by $\leq 40 Mpc/h$ (red), $50 Mpc/h$ (blue), and $60 Mpc/h$ (magenta), with 21940, 37282, and 58675 cluster pairs respectively. In these $10 Mpc/h$ radius cylinders around cluster pairs, the fraction of halos relative to all is noted at left, the fraction of pixels with halos, relative to all with halos, at right. Bottom panels: some self similarity is seen when dividing each curve by its peak (distance=0) value. The high mass ($> 10^{13} M_{\odot}$) halo counts and mass density profiles do not increase towards the filaments as much as the profiles which include lower mass halos.

the $1/r^2$ profile for visually detected filaments found by Colberg, Krugman & Connolly (2005) (also fit starting around $2 Mpc/h$). This might indicate some issue with the assigned filaments, either in how they are chosen, or the fact that filaments are taken to be straight between any pair of clusters, which might be washing out some of the radial structure. In the Colberg, Krugman & Connolly (2005) filament catalogue, only 38% of the filaments were straight lines between the cluster endpoints.

As the cluster pairs with filaments tend to have similar shape profiles in the 36 different combinations, one can characterize the filament profiles by peak values relative to the

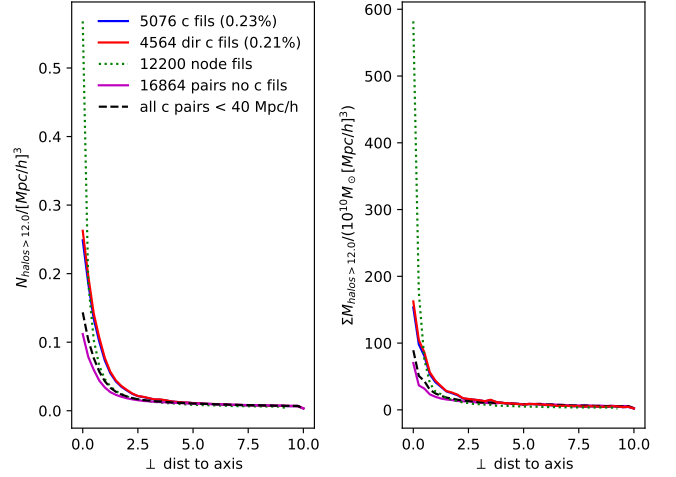


Figure 12. Example of the radial galaxy number density (left) and halo mass density (right) perpendicular to the line linking all $\leq 40 Mpc/h$ pairs of neighboring DISPERSE nodes (dotted line), clusters connected by filaments either directly (“dir c”, red solid line) or also via interpolation (“c”, blue solid line), not connected by filaments (bottom magenta line) and average (dashed, same curve as in Fig. 11). This is for $10^{12} M_{\odot}$ halos around cluster pairs separated by up to $40 Mpc/h$, using the “patch” method for matching clusters to DISPERSE nodes, and underlying $2 Mpc/h$ DISPERSE web with 3σ persistence. Other choices of matching, persistence and smoothing are similar, with enhancement near the origin, see Fig. 13 below, being the largest variation between them.

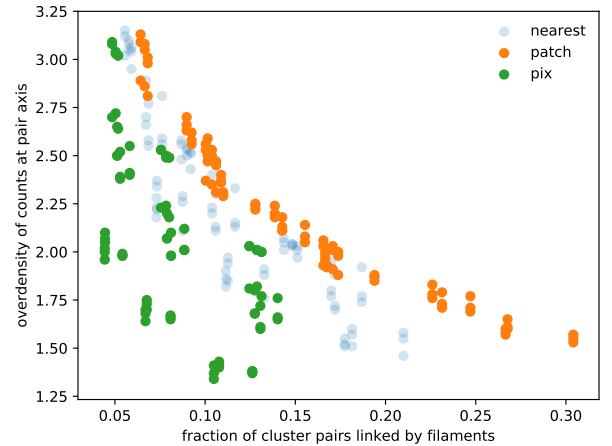


Figure 13. Ratio of the enhancement of the filament profile peak over the average pair profile peak for the different filament pairs as a function of fraction of all cluster pairs in the 36 combinations. The general trend within a matching method is that the more pairs with filaments, the less enhancement there is of the peak density over the average. Points towards the right (higher fraction of pairs linked by filaments) are for the shorter maximum lengths, those towards the top (higher overdensity at peak) are for smaller smoothing.

peak average of all cluster pairs with the same maximum pair separation and using the same minimum halo mass. The distribution of this enhancement is shown as a function of the fraction of cluster pairs linked by filaments in Fig. 13. As most of the cluster pairs don't have filaments, the difference between profiles for the unlinked cluster pairs and all cluster pairs for maximum lengths $\geq 40 \text{ Mpc}/h$ is small. The fraction of cluster pairs which have filaments goes down with increasing maximum cluster separation, as well as with more restrictive ways of matching clusters to filaments, ranging from $\sim 30\%$ of the pairs for “patch” and one of the $40 \text{ Mpc}/h$ separations, to from 2% of the pairs for “pix” and one of the $60 \text{ Mpc}/h$ separation, roughly integrals of the distributions shown in Fig. 9. There tends to be less density enhancement relative to all pairs as the fraction of pairs which are filaments increases, as is expected, and the enhancement also tends to be lower for the “pix” matching and highest for the “patch” matching, as can be seen in Fig. 13.

On average, cluster pairs with filaments assigned via this method were a relatively small fraction of close pairs. Nonetheless, the average density along the line between all pairs, up to a certain separation, was enhanced by a factor of around 10 relative to a position $\sim 10 \text{ Mpc}/h$ away from the line connecting the cluster pair. Pairs with filaments assigned for any of the 36 combinations considered in more detail had maximum enhancement ranging from ~ 1.25 to 3.25 of the average.

4.3 DISPERSE node pair filaments

Also shown in Fig. 12 are filament profiles in density counts and in halo mass density for DISPERSE node pairs in the underlying DISPERSE web. There are several uncertainties and subtleties in calculating DISPERSE filament profiles. The DISPERSE node filaments are assumed to run straight between the two nodes, discarding the shape information provided by DISPERSE. In addition, the DISPERSE nodes are defined for pixel ($2 \text{ Mpc}/h$ side) averaged densities, so that actual density peaks, if present, might be anywhere in the pixel, and are likely offset with respect to the few discrete positions the DISPERSE nodes take. In practice, the DISPERSE filament node pair profiles are stacked just as those for cluster pairs, and then the peak in the density perpendicular to the line connecting the DISPERSE nodes is shifted to be at the origin.

However, the lack of resolution for the DISPERSE node position also causes another complication. Calculating the overdensity by stacking just as for clusters, the DISPERSE node pair total halo mass density peak is enhanced, relative to the cluster filament pairs, by almost a factor of 10 within about $2 \text{ Mpc}/h$, while the counts density is not (closer to a factor of ~ 2). One reason appears to be that a significant fraction of the DISPERSE nodes have a cluster within $2 \text{ Mpc}/h$ (a similar fraction to the number with a cluster in the same pixel, see the stars in Fig. 5). This cluster possibly would correspond to the filament endpoint in “reality”, but the mass density average in each pixel, in the original input to DISPERSE, loses this information. In the profiles of cluster-cluster pairs, the mass of the endpoint clusters was not included, but in the Disperse node-node pairs, this endpoint mass is included automatically. In order to try to take this effect out, the nearest cluster within $2 \text{ Mpc}/h$ of the DISPERSE node was taken

out of the mass profile sum. The resulting density profiles are what are plotted for the DISPERSE filament profiles in Fig. 12.

Even with the smoothing expected from the resolution noise constraint, expected to lower the overdensity peak somewhat, the central density counts for, e.g., $2 \text{ Mpc}/h$ smoothing and 3σ persistence, were enhanced by around a factors of 2-6 over the corresponding cluster filament pairs, and for the mass in halos above a given cutoff, there is another enhancement, for the DISPERSE node filaments of $\sim 1 - 2$.

The DISPERSE filament peak overdensity counts depended more on persistence than pair separation (unlike the clusters), with lower persistence leading to a lower central density. The higher overdensity of halos and halo mass between DISPERSE node filament pairs compared to cluster filament pairs may be due to the automatic linking of cluster pairs when cluster-DISPERSE node matching gave more than one match or the possibility of washing out of the peak position by the matching method to clusters. Further exploring this is beyond the scope of this note, however.

5 SUMMARY AND DISCUSSION

Here, the largest mass halos in the universe, clusters $10^{14} M_{\odot}$ and above, were matched to nodes in cosmic webs created using the web finder DISPERSE on pixel overdensities in a fixed time N-body simulation box. Filaments between cluster matched DISPERSE nodes were assigned to their corresponding cluster pairs.

DISPERSE was chosen because of its public availability and its frequent use, and applied to 4 smoothings of the underlying dark matter, the largest of which ($5 \text{ Mpc}/h$) matched too poorly to clusters to be studied in much detail. For the remaining smoothings, 3 values of the DISPERSE persistence parameter were considered, resulting in 9 different DISPERSE webs based upon the same simulation.

In each of these 9 webs, clusters were matched to nodes by assigning a volume to the DISPERSE nodes via 4 methods, and then seeing if the cluster lay within this volume. Volumes were given by the DISPERSE node pixel ($\sim 2 \text{ Mpc}/h$), a twice smoothing radius sphere around the DISPERSE node, or within the same Hessian node “patch” (contiguous pixels all classified as nodes via the Hessian method). No method matched every cluster to a DISPERSE node, but about half of the clusters had a matched DISPERSE node for every method, in all 9 underlying DISPERSE webs, and 3/4 had matches if the most restrictive matching (lying in the same pixel) was dropped. The clusters matched to DISPERSE nodes for the most methods and underlying DISPERSE webs tended to have higher mass and lower “velocity shear”, and, perhaps a higher likelihood of recent 1:3 mergers. High density DISPERSE nodes were more likely to have a matched cluster.

For every DISPERSE web, there generally appeared to be a distinct population of clusters “near” the DISPERSE nodes, and for clusters and their nearest DISPERSE nodes within twice the smoothing length of each other, a cluster mass-DISPERSE node density relation is seen.

Filaments between DISPERSE node pairs which each have a matched cluster can be assigned to the corresponding cluster pair; a method for interpolating filaments through unmatched DISPERSE nodes was also applied. For 10% -25% of clusters there are no filaments to other clusters with DIS-

PERSE node matches, either because they had no matching DISPERSE node (and thus do not have any DISPERSE node's filaments) or because their cluster matched DISPERSE nodes were not linked to any other cluster matched DISPERSE node. Only 47 of the clusters (out of 2898) never had a filament for any of the underlying DISPERSE webs and matching methods (152 clusters if one didn't interpolate filaments when dropping unmatched DISPERSE nodes). Closer cluster pairs were more likely to be linked by such filaments, although some of the matching methods showed a dip in this probability between 5-10 Mpc/h . Beyond 15-20 Mpc/h separations, pairs with filaments were a minority of cluster pairs (but around half of the cluster filament pairs were at larger separations). Cluster pairs with the long axis of one cluster aligned with the direction of the cluster pair also made the cluster pair more likely to be linked by a filament, and "importance" from an out of the box machine learning method also found that cluster-cluster long axis alignments made an intervening filament more likely, as expected from other studies. The halo and halo mass density around cluster pairs is enhanced, with more enhancement for the average profile of pairs connected by these filaments. The profile away from the filament pair was $1/r$, weaker than the $1/r^2$ falloff beyond 2 Mpc/h , as found in e.g. Colberg, Krugman & Connolly (2005), perhaps due to assuming the filaments were straight lines between the pairs, but also possibly due to how filaments are defined from the underlying web. Unlike the cluster-DISPERSE node matching, where many clusters had DISPERSE node matches for the whole set of underlying DISPERSE webs and matching methods, most cluster pairs only had filaments for a few of the underlying DISPERSE web and matching methods.

This matching between clusters and the cosmic web picks out subclasses of both, clusters and cluster pairs, which have corresponding DISPERSE nodes and filaments, and those which do not. Some trends in unmatched clusters were seen, others might be present as well, perhaps either in the dark matter properties or observable properties of these clusters. Unfortunately, the more recent galaxy formation models built upon the Millennium simulation are only for the rescaled (Angulo & White 2010; Angulo & Hilbert 2015) Millennium simulation, for which smooth particle densities were not available. It would be interesting to study these different kinds of clusters in a simulation incorporating what is now known about current galaxy observables.

The unmatched DISPERSE nodes tended to be less massive but not always; those in the higher mass range, where sometimes there is a cluster match and sometimes there isn't, would also be interesting to better understand. For example, nodes also can be evaluated in terms of other properties such as their histories (Cadiou et al 2020), just as clusters are. To catch more of the DISPERSE nodes, it is of course possible to go down to lower halo mass and do the matching procedure again. This will likely increase the number of clusters which have an associated filament to either a cluster or a lower mass halo.

The clusters also give a reference point with which to compare nodes between different webs. That is, as 3/4 of the clusters had DISPERSE node matches for the all 9 webs, and for "nearest", "fixed", and "patch" matching methods, the DISPERSE nodes they match to can be intercompared. This could also be done for other webs, as a way to identify corresponding nodes.

In this approach, cluster-cluster filament pairs are a particular selection of all the cluster pairs, and different underlying DISPERSE webs resulted in different cluster pairs being assigned filaments. Unlike clusters-DISPERSE node matching, where many clusters always had matches, fewer than 10% of the cluster pairs which ever had a filament had one among most of the different webs and matching methods, this fraction dropped by a factor of 2 if interpolation through dropped DISPERSE nodes was dropped. It would be interesting to see how much overlap there is in filaments found between clusters for other constructions which also have some sort of node-cluster identification (or have clusters defined as nodes directly).

At least for the methods of assigning filaments to cluster pairs here, whether a cluster pair shares a filament depends upon which web definition is of interest, which is a question which comes from outside of the cluster-DISPERSE node correspondence. It would be interesting to see how much variation occurs if clusters are matched to nodes and then assigned filaments in other web definitions. One might use some of these differences between cluster filament pair properties (denser filament profile, or higher likelihood of nearby pairs being connected) as ways to characterize different, and maybe select, web finders, depending upon the application in mind.

Clusters are very important gravitationally bound objects in the universe, and special environments in galaxy formation, while nodes anchor the cosmic web which evolves as structure forms. The connection between the two provides a way to better understand clusters, cosmic web nodes, and their relation and evolution together.

ACKNOWLEDGEMENTS

Many thanks especially to K. Kraljic and M. White for numerous discussions and suggestions, and to M. Alpaslan, S. Codis, C. Laigle, C. Pichon, A. White, for help as well, and to the participants of the Higgs 2019 Cosmic Web meeting, and the CCA, CERN, IAP, NYU, and the Royal Observatory of Edinburgh for hospitality and opportunities to present and discuss this work. I am also grateful for the Millennium simulation database.

REFERENCES

- Alpaslan M., et al, 2014, MNRAS, 438, 177
- Angulo R.E., White S.D.M., 2010, MNRAS, 405, 143
- Angulo R.E., Hilbert S., 2015, MNRAS, 448, 364
- Aragon-Calvo M. A., Jones B. J. T., van de Weygaert R., van der Hulst J. M., 2007, A&A, 474, 315
- Bardeen J. M., Bond J. R., Kaiser N., Szalay A. S., 1986, ApJ, 304, 15
- Barrow J. D., Bhavsar S. P., Sonoda D. H. 1985, MNRAS, 216, 17
- Bond J.R., Kofman L., Pogosyan D., 1996, Nature, 380, 603
- Bond J.R., Myers S.T., 1996, ApJ Suppl.103, 1
- Bos E.G.P., 2016, PhD Thesis.
- Bos E.G. P., van de Weygaert R., Kitaura F., Cautun M., 2016, the Zeldovich Universe: Genesis and Growth of the Cosmic Web, Eds, R. van de Weygaert, S.F.Shandarin, E. Saar, J. Einasto, 2014 conference, arxiv: 1611.01220
- Cadiou C., Pichon C., Codis S., Musso M., Pogosyan D., Dubois Y., Cardoso J. -F., Prunet S., 2020, MNRAS, 496, 4787

- Cautun M., van de Weygaert R., Jones B. J. T., 2013, MNRAS, 429, 1286
- Cautun M. van de Weygaert R., Jones B.J.T., Frenk C.S., 2014, MNRAS, 441, 2923
- Codis S., Pichon C., Pogosyan D., 2015, MNRAS, 479, 973
- Colberg J.M., Krughoff K.S., Connolly A., 2005, MNRAS, 359, 272
- Falck B., Neyrinck M. C., 2015, MNRAS, 450, 3239
- Falck B. L., Neyrinck M. C., Szalay A. S., 2012, ApJ, 754, 12
- Fang F., Forero-Romero J., Rossi G., Li X.-D., Feng L. L., 2019, MNRAS, 485, 5276
- Forero-Romero J. E., Hoffman Y., Gottlober S., Klypin A., Yepes G., 2009, MNRAS, 396, 1815
- Hahn, O., Porciani, C., Carollo, C.M., Dekel, A., 2007, MNRAS, 375, 489
- Hahn O., Carollo C. M., Porciani C., Dekel A., 2007b, MNRAS, 381, 41
- Hellwing W.A., Cautun M., van de Weygaert R., Jones, B.T., 2021, arXiv:2011.08840
- “The Cosmic Web: From Galaxies to Cosmology”, 2019, Royal Observatory, Edinburgh, slides at: <https://higgs.ph.ed.ac.uk/workshops/the-cosmic-web-from-galaxies-to-cosmology/>
- Kraljic K., et al, 2019, MNRAS, 483, 3227
- Laigle C., et al, 2015, MNRAS, 446, 2744
- Leclercq F., Lavaux G., Jasche J., Wandelt B., 2016, JCAP, 08, 027
- Lemson, G., Springel, V., 2006, *Cosmological Simulations in a Relational Database: Modelling and Storing Merger Trees*, Astronomical Data Analysis Software and Systems XV, Eds., Astronomical Society of the Pacific Conference Series, 351, 212
- Libeskind N.I., et al, 2018, MNRAS, 473, 1195
- Ludlow A.D., Porciani C., 2011, MNRAS, 413, 1961
- Park D., Lee J., 2009, MNRAS, 397, 2163
- Pereyra L.A., Sgro M.A., Merchan M.E., Stasyszyn F.A., Paz D.J., 2020, MNRAS, 499, 4876
- Planck collaboration, Aghanim N., Akrami Y., Ashdown M., Aumont J., et al, A&A, 2020, 641, A6
- Pogosyan D., Bond J.R., Kofman L., 1998, JRASC, 92, 313
- Ramachandra N. S., Shandarin S. F., 2015, MNRAS, 452, 1643
- Rost A., Stasyszyn F., Pereyra L., Martinez H.J., 2019, arXiv:1911.08545, “A comparison of cosmological filaments catalogues”
- Shandarin S., Zel’dovich Y., 1989, Rev. Mod. Phys., 61, 185
- Shandarin S. F., 2011, J. Cosmology Astropart. Phys., 5, 15
- Sousbie T., 2011, MNRAS, 414, 350
- Sousbie T., Pichon C., Kawahara H., 2011, MNRAS, 414, 0384
- Springel V., et al, 2005, Nature, 435, 629
- van de Weygaert R., Bond J.R., 2008, A Pan-Chromatic View of Clusters of Galaxies and the Large-Scale Structure, Lecture Notes in Physics, Volume 740. ISBN 978-1-4020-6940-6. Springer Science+Business Media B.V., 2008, p. 335
- van de Weygaert R., Shandarin S., Saar E., Einasto J., eds, 2016, The Zeldovich Universe: Genesis and Growth of the Cosmic Web IAU Symposium Vol. 308, doi:10.1017/S174392131601098X
- Wang P., Kang X., Libeskind N., Guo Q., Gottlober S., Wang W., 2020, New Ast. 80, 101405
- Winkel N., Pasquali A., Kraljic K., Smith R., Gallazzi A.R., Jackson T.M., 2021, arXiv:2105.1336
- Zel’dovich Y. B., 1970, A&A, 5, 84